



Kinetic studies on the pyrolysis of pinewood

Garima Mishra, Jitendra Kumar, Thallada Bhaskar*

Thermo-catalytic processes area (TPA), Bio-Fuels Division (BFD), CSIR-Indian Institute of Petroleum (IIP), Dehradun 248005, India



HIGHLIGHTS

- Model free kinetic studies on pyrolysis of pine wood.
- Determination of kinetic triplet from TG analysis using isoconversional methods.
- Prediction of kinetic mechanism using master plots and compensation effect.
- Isothermal predictions from non-isothermal data for validation of kinetic results.

ARTICLE INFO

Article history:

Received 10 October 2014

Received in revised form 21 January 2015

Accepted 22 January 2015

Available online 11 February 2015

Keywords:

Pyrolysis

Model free

Master plots

Compensation

Kinetic studies

ABSTRACT

The kinetic study for pyrolysis of pine wood has been studied by a thermogravimetric analyzer in an inert atmosphere. Non isothermal model free kinetic methods were used to evaluate kinetics at six different heating rates of 5–40 °C/min. Three zones can be detected from the iso-conversional plot of pine with average activation energy values of 134.32 kJ/mol, 146.89 kJ/mol and 155.76 kJ/mol in the conversion range of 1–22%, 24–84% and 85–90%, respectively. The activation energy values were used to determine the reaction mechanism using master plots and compensation parameters. The results show that the pyrolysis process of pine wood can be described by two dimensional diffusion reaction mechanism in a wide range of conversion up to 0.7, followed by close to one and half order reaction mechanism. The kinetic results were validated by making isothermal predictions from non-isothermal data.

© 2015 Elsevier Ltd. All rights reserved.

1. Introduction

Biomass is a renewable resource, whose utilization has received great attention due to environmental considerations and the increasing demands of energy worldwide (Tsai et al., 2007). Biomass resources include wood and wood wastes, agricultural crops and their waste byproducts, municipal solid waste, animal wastes, waste from food processing, and aquatic plants and algae. Pyrolysis is one of the thermochemical biomass conversion methods with best industrial perspectives for biomass valorization, since the process conditions can be optimized to maximize the yields of gas, liquid and char (Czernik and Bridgwater, 2004). The pyrolysis behavior of lignocellulosic biomass depends on its three major building blocks: cellulose, hemicellulose and lignin. Forest biomass contains a high weight percentage of cellulose and lignin, whereas agricultural biomass contains a high weight percentage of cellulose and xylan (Cendrowska, 1997). Hardwoods have a higher proportion of cellulose and xylan than softwoods. The varying proportions of three key components affect the pyrolysis behavior of biomass

feedstocks and affect the yields of pyrolysis products both quantitatively and qualitatively.

Thermal analysis techniques such as thermogravimetric analysis (TGA) have been widely used to study biomass kinetics as they are high-precision methods and provide quantitative methods for examination of processes and estimation of effective kinetic parameters for various decomposition reactions. The actual reaction scheme of wood pyrolysis is extremely complex because of the formation of over a hundred intermediate products. The pyrolysis of wood is, therefore, generally modeled on the basis of apparent kinetics (Di Blasi, 2008). Numerous works on kinetic studies of wood have been reported in literature (Koufopoulos et al., 1989; Matheus et al., 2012; Sbirrazzuoli, 2013; Tsai et al., 2007). Bamford et al. (1946) reported the first model of pyrolysis based on a single reaction scheme with first order kinetics. Di Blasi (2008) presented a review of the various studies on modeling of chemical and physical processes of biomass pyrolysis reported in literature. A majority of kinetic mechanisms consists of a single or three parallel reactions for the formation of the main product classes (one-stage or one-component mechanisms) following the proposal by Shafizadeh and Chin (1977) for wood (Di Blasi, 2008). These models come under the model fitting approach of

* Corresponding author. Tel.: +91 135 2525820; fax: +91 135 2660202.

E-mail addresses: tbhaskar@iip.res.in, thalladab@yahoo.com (T. Bhaskar).

kinetic analysis which suffers from several drawbacks. The forcible fitting of data leads to ambiguous kinetic predictions where more than one kinetic mechanism are likely to give good fits for same set of data. The most important feature of a reliable method of kinetic analysis is its ability to handle multi step processes (Vyazovkin, 2000). The isoconversional analysis provides a fortunate compromise between the oversimplified but widely used single step Arrhenius kinetic treatment and the prevalent occurrence of processes whose kinetics are multi-step and/or non-Arrhenius (Vyazovkin and Sbirrazzuoli, 2006). These methods allow estimates of the apparent activation energy at progressive degrees of conversion.

This paper focuses on determining the characteristics and kinetics that describes the thermal decomposition process of pine wood. The pyrolysis behavior of pine wood is studied using a thermogravimetric analyzer and the kinetic predictions are made using the non-isothermal model free kinetic methods. Generalized master plots and method of compensation effect are used to deduce the reaction mechanism governing the decomposition process. The selected methods for analyzing solid state kinetic data for pine wood pyrolysis are compared. The understanding of process is realized through kinetic equations that provides basis for further applications of the thermochemical conversion of pine wood as a potential feedstock.

2. Experimental method

2.1. Sample preparation and characterization

The pine wood sample used in the study was dried at room temperature. It was ground and sieved to an average particle size of 50 μm . The ultimate analysis of pine wood sample showed that it contains 47.2% C, 7.7% H, and 44.9% O. It contains very less amount of sulfur (0.029%). The calorific value of pine sample was 17.34 MJ/kg, measured using a Parr 6300 bomb calorimeter. Proximate analysis of sample showed that it contains 13.58% moisture and about 95% volatiles (wet basis). It has a very less ash content of 0.835%. Moisture content of the feed has been obtained from the HR-83 Mettler Toledo Halogen Moisture Analyzer.

The trace metal analysis of pine sample has been carried out in the DRE, PS-3000 UV, Leeman Labs Inc., Inductively Coupled Plasma-Atomic Emission Spectroscopy. A high content of Potassium (1491 ppm), Calcium (841 ppm), and Phosphorus (314 ppm) is found in the sample with traces of Sodium, Iron, Aluminum, Zinc, etc.

2.2. Experimental techniques

The thermogravimetric analysis was carried out in DTG-60 unit (Shimadzu, Japan). Pine samples of average particle size of 50 μm were taken in alumina crucibles with sample mass in the range of ca. 10 mg and were heated from room temperature to 700 $^{\circ}\text{C}$ at six different heating rates of 5, 10, 15, 20, 30 and 40 $^{\circ}\text{C}/\text{min}$. Nitrogen gas at a flow rate of 100 ml/min was used as an inert purge gas to displace air in the pyrolysis zone, thus avoiding unwanted oxidation of the sample. The experimental results were tested to ensure repeatability.

3. Evaluation of pre-exponential factor and reaction mechanism $f(\alpha)$ for model free methods

A kinetic analysis is incomplete without the determination of pre-exponential factor and reaction mechanism. The analysis of E_{α} dependencies helps in predicting kinetics and exploring the mechanisms of processes. Several methods have been proposed for evaluation of these parameters. A brief description of the methods used in the present study is as follows:

3.1. Using compensation parameters

Lesnikovich and Levchik (1983) reported that an apparent compensation effect is observed when a model fitting method is applied to a single-heating rate run. This compensation effect can be used for elucidating the reaction mechanism of the process using different reaction models. Substitution of different models $f(\alpha)$ into a rate equation (Eq. (3)) and fitting it to experimental data yields different pairs of the Arrhenius parameters, A_i and E_i . The models $f(\alpha)$ used in evaluation are given in Table 1. Eq. (3) has been provided in Supplementary information.

Table 1
Expressions for $f(\alpha)$ and $g(\alpha)$ functions for some of the common mechanisms operating in solid state reactions.

S. No.	Model	Differential form $f(\alpha)$	Integral form $g(\alpha)$
Nucleation models			
P2	Power law	$(2/3) \alpha^{-1/2}$	$\alpha^{3/2}$
P3	Power law	$2\alpha^{1/2}$	$\alpha^{1/2}$
P4	Power law	$3\alpha^{2/3}$	$\alpha^{1/3}$
P5	Power law	$4\alpha^{3/4}$	$\alpha^{1/4}$
Sigmoidal rate equations			
A1	Avrami-Erofeev	$(3/2) (1 - \alpha) [-\ln (1 - \alpha)]^{1/3}$	$[-\ln (1 - \alpha)]^{2/3}$
A2	Avrami-Erofeev	$2(1 - \alpha) [-\ln (1 - \alpha)]^{1/2}$	$[-\ln (1 - \alpha)]^{1/2}$
A3	Avrami-Erofeev	$3(1 - \alpha) [-\ln (1 - \alpha)]^{2/3}$	$[-\ln (1 - \alpha)]^{1/3}$
A4	Avrami-Erofeev	$4(1 - \alpha) [-\ln (1 - \alpha)]^{3/4}$	$[-\ln (1 - \alpha)]^{1/4}$
F1	Prout-Tompkins	$\alpha(1 - \alpha)$	$\ln [\alpha/(1 - \alpha)]$
F2	Contracting area	$2(1 - \alpha)^{1/2}$	$1 - (1 - \alpha)^{1/2}$
F3	Contracting volume	$3(1 - \alpha)^{2/3}$	$1 - (1 - \alpha)^{1/3}$
F4	Random nucleation (1)	$(1 - \alpha)^2$	$1/(1 - \alpha)$
F5	Random nucleation (2)	$(1 - \alpha)^3/2$	$1/(1 - \alpha)^2$
Diffusion models			
D1	1D diffusion	$1/2\alpha$	α^2
D2	2D diffusion-Valensi	$[-\ln (1 - \alpha)]^{-1}$	$(1 - \alpha) \ln (1 - \alpha) + \alpha$
D3	3D diffusion-Jander	$(3/2) (1 - \alpha)^{2/3} / [1 - (1 - \alpha)^{1/3}]$	$[1 - (1 - \alpha)^{1/3}]^2$
D4	3D diffusion-Ginstling	$(3/2) / [(1 - \alpha)^{-1/3} - 1]$	$1 - 2\alpha/3 - (1 - \alpha)^{2/3}$
Reaction order models			
R1	First order	$1 - \alpha$	$-\ln (1 - \alpha)$
R2	Second order	$(1 - \alpha)^2$	$(1 - \alpha)^{-1} - 1$
R3	Third order	$(1 - \alpha)^3$	$[(1 - \alpha)^{-2} - 1]/2$
R6	One and half order	$(1 - \alpha)^{3/2}$	$2[(1 - \alpha)^{-1/2} - 1]$

Although the parameters vary widely with the selected model $f(\alpha)$, they all demonstrate a strong correlation known as a compensation effect:

$$\ln A_i = \alpha^* + \beta^* E_i \quad (14)$$

where α^* and β^* are constants (the compensation effect parameters). For each heating rate, β_v , using an integral or differential method, the pairs (A_{vj}, E_{vj}) , characteristic for each conversion function $f(\alpha)$, are determined using any form of equation (differential or integral). Using the relation of the apparent compensation effect, for each heating rate the compensation parameters (α_v^* , β_v^*) are determined. Now using these compensation parameters (α_v^* , β_v^*) the A_x is obtained at using E_x values at each conversion value.

$$\ln A_x = \alpha^* + \beta^* E_x \quad (15)$$

The parameters E and $\ln A$ obtained by the model-fitting procedure are only used here to evaluate the relationship that exists between E and $\ln A$. The objective of this method is not to give an interpretation of the compensation effect and its origins remain the subject of debate. If a compensation effect is observed, then the above method can be used to compute a model-free value of $\ln A_x$ for each value of E_x obtained by means of an isoconversion method (Sbirrazzuoli, 2013). When A_x and E_x values are obtained at each conversion value $f(\alpha)$ can be obtained numerically by putting the values of A_x and E_x in Eq. (1). Eq. (1) has been provided in Supplementary information.

3.2. $z(\alpha)$ master plots

The $z(\alpha)$ plots are derived by combining the integral and differential forms of reaction model.

$$z(\alpha) = f(\alpha) * g(\alpha) \quad (16)$$

$$z(a) = \frac{d\alpha}{dt} \exp\left(\frac{E_x}{RT_x}\right) \int_0^{T_x} \exp\left(\frac{-E_x}{RT}\right) \quad (17)$$

The temperature integral is approximated by fourth rational expression of Senum-Yang approximation. The temperature integral solved using trapezoidal rule yields less errors in comparison with Senum-Yang approximation, which proves that Senum Yang approximation yields good values at lesser computation. The

theoretical and experimental $z(\alpha)$ curves are compared and the best fit model is determined. Once the reaction model is identified the pre-exponential factor is also determined from any of the integral or differential rate expression.

4. Results and discussion

4.1. Thermogravimetric analysis (TGA)

The TG and DTG curves of pine wood in inert atmosphere of nitrogen at different heating rates are shown in Figs. 1a and 1b, respectively.

Three zones can be identified for the pyrolysis process of pine from the TG curves. In the first zone, with a temperature range from ambient to around 150 °C, a slight weight loss of 10.152% can be seen in this zone. This weight loss is due to removal of moisture and some light volatile compounds. The main decomposition occurs in the second stage which is also known as the active pyrolysis zone and corresponds to the temperature range of 150 °C to 400 °C. The deconvolution of DTG curve (Fig. 1c) shows two visible peaks in this zone which can be related to hemicellulose and cellulose decomposition with peak maxima at temperatures of 323.12 °C and 359.16 °C, respectively. The merged peaks of hemicellulose and cellulose form a broader peak for the second region. The third zone corresponds to temperature range of 400–700 °C and is referred as the passive pyrolysis zone where continuous slight devolatilization takes place, lignin decomposition being the most prominent reaction in this region. This zone is associated with a weight loss of 11.685%. At the temperatures above 400 °C, the final decomposition involves the aromatization process of lignin fraction leading to very low weight loss (Fisher et al., 2003). A wide peak for lignin decomposition in temperature range of 220 °C to 700 °C can be seen from the deconvoluted DTG curve. Lignin decomposes slowly over a wide temperature range (in both active and passive pyrolysis regions) and is responsible for the long tailing of DTG curve. Pine wood undergoes a total decomposition of 83.3% till 900 °C.

TG and DTG curves of pine wood were recorded at six different heating rates of 5, 10, 15, 20, 30, 40 °C/min, respectively. Figs. 1a and 1b shows the effect of heating rate on TG and DTG curves. As the heating rate increases, the maximum DTG value increases and the DTG curve shifts to higher temperature range. When heating rate increases, starting and final temperature of active

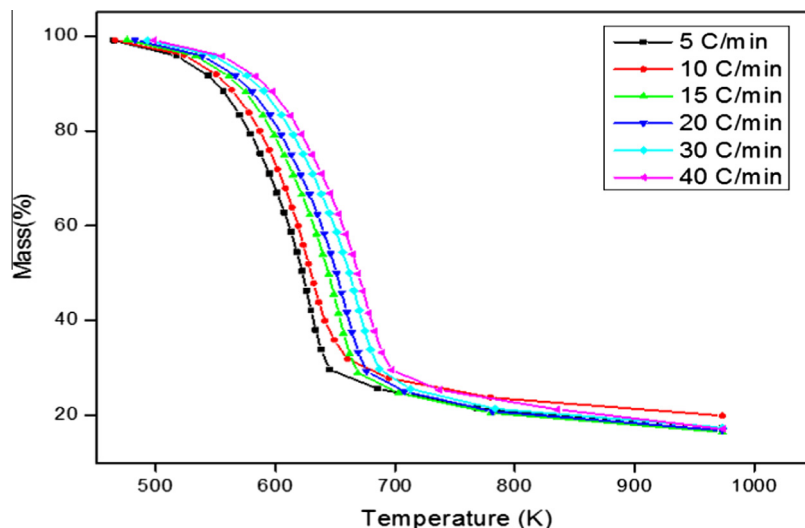


Fig. 1a. TG curves of pine at different heating rates.

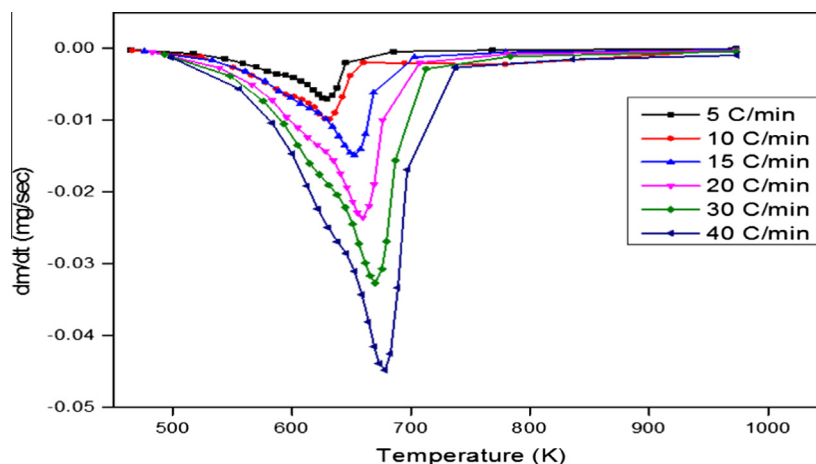


Fig. 1b. DTG curve of pine at different heating rates.

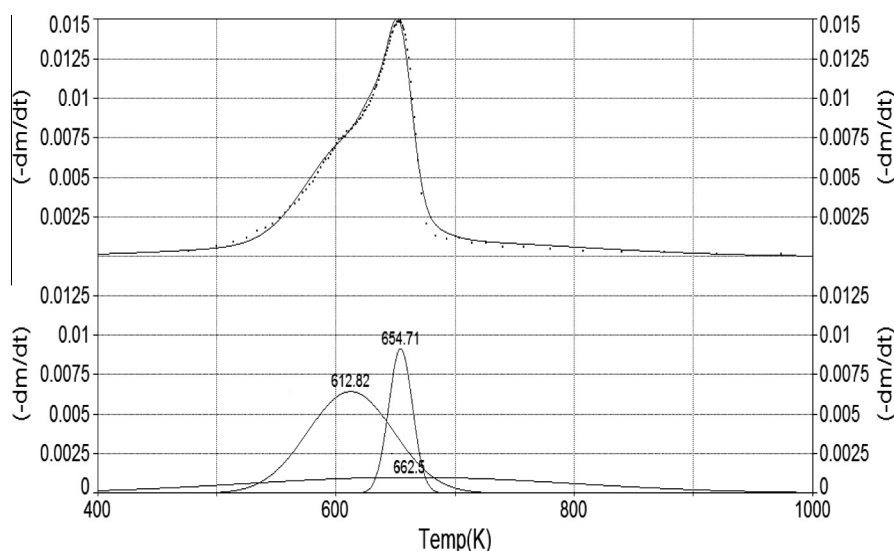


Fig. 1c. Deconvolution of DTG curve of pine at 10 °C/min

and passive pyrolysis region also increase. This can be due to heat and mass transfer limitations. Temperature gradients may exist in the particle, because of heat transfer limitations due to which the temperature in the core of a particle can be a bit lower than temperature on its surface. (Milosavljevic and Suuberg, 1995) Thus this can be due to the reduced efficiency of heat transfer at higher heating rates than at lower heating rates.

4.2. Kinetic analysis results

The thermograms recorded for pine wood at six different heating rates (5, 10, 15, 20, 30 and 40 °C/min) were used with above mentioned model-free methods to calculate the kinetic parameters. The conversion range up to 90% was taken as the kinetic analysis range for each heating rate to obtain the isoconversion plot of activation energy E_a with conversion α . The step size of 0.01 is selected as per the recommendations of ICTAC Kinetics Committee, (Vyazovkin et al., 2011) to detect and treat the multi-step kinetics. The temperature range for kinetic studies is taken as 150–700 °C as at temperatures less than 150 °C only moisture and physically absorbed water is removed and there is almost negligible weight loss after 700 °C. The plots for Friedman method, KAS

method and FWO method are shown in Figs. S1, S2 and S3 (refer Supplementary information). All the plots show high correlation coefficients (R) greater than 0.98 and give good fit to the experimental data. Fig. 2 gives the isoconversional plots of apparent activation energy versus conversion for the selected methods.

The trend of activation energy versus conversion plot is similar for all the kinetic analysis methods taken. As can be seen from the isoconversional plots of pine wood, the activation energy varies with conversion but the variation is not dramatically large. The small differences among the activation energy values determined by means of different isoconversional methods are due to the different approximations used to calculate the temperature integral in these methods. The activation energy values obtained by Friedman method are greater than the values estimated by other kinetic analysis methods. The curves for KAS, FWO and Vyazovkin are almost overlapping with similar trend. Vyazovkin AIC method gives a slightly irregular isoconversional curve with activation energy values fluctuating along the plot for other methods. The Friedman method represents an efficient method for evaluation of activation energy as it involves no oversimplified approximation and is based on the simple differential form of kinetic rate law. One major drawback of Friedman method is that it is a differential method, which can be applied to integral data (e.g. TG data) only

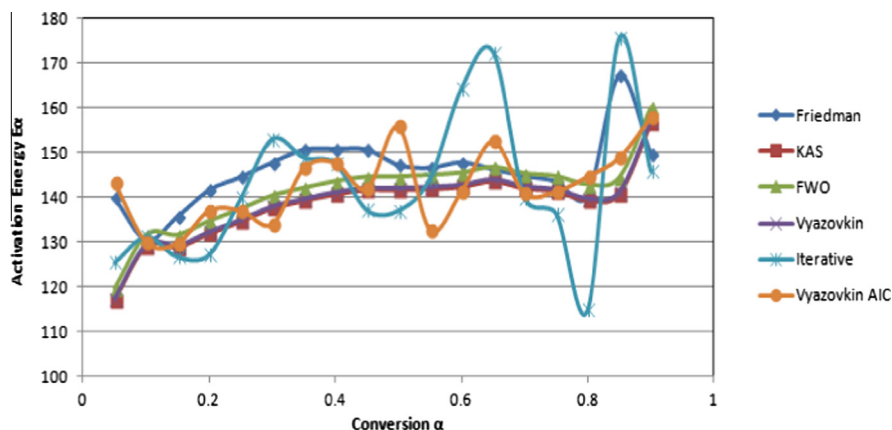


Fig. 2. Isoconversion plots for activation energy versus conversion.

after numerical differentiation of experimental α versus T curves that tends to yield quite noisy rate data and, therefore, scattered E_a values. In the present study the isoconversional plot of Friedman method is regular without any erratic values of activation energy except at conversion values greater than 0.9. The KAS, FWO methods give a smooth and overlapping isoconversional curve but the use of oversimplified approximations in the methods to form the kinetic equations, make these methods uncertain and inaccurate. The KAS uses the simple approximation for exponential integral i.e. $p(x) = \exp(-x)/x^2$ and FWO method uses the linear Doyle's approximation to evaluate the temperature integral. Vyazovkin's method employs the fourth rationale Senum-Yang approximation for temperature integral which gives very less errors and hence can be used efficiently. Vyazovkin's method leads to activation energy values very close to KAS and FWO method due to the undesirable flattening of E_a versus α curve caused by averaging of values in evaluation of integral from 0 to α . Vyazovkin AIC method modifies and increases the accuracy of Vyazovkin method by taking the constancy of activation energy for a small segment $\Delta\alpha$. Trapezoidal rule is used in this paper for evaluation of temperature integral in Vyazovkin AIC method. The iterative linear method was evaluated up to 4 iterations until which it converged to final values of activation energies. Iterative method gave fluctuating values in comparison with the other methods. The activation energy values obtained from Friedman methods seem to give best fit for the thermogravimetric data of pine wood. The variation of apparent activation energy with conversion indicates occurrence of a complex multistep mechanism for pine wood pyrolysis. This variation helps in detecting the reaction model and pre exponential factor. Closely looking at the dependence of activation energy on conversion three regions can be detected from the curve. In the first region ($0.1 < \alpha < 0.22$) the activation energy values gradually increases from 104 to 143.54 kJ/mol with an average value of 134.213 kJ/mol. In the second region ($0.23 < \alpha < 0.84$) the values of apparent activation energy are almost constant and vary in a small range of 140.34–151.17 kJ/mol with an average value of 146.89 kJ/mol. In the third region ranging from $0.85 < \alpha < 0.9$ the activation energy values show a marked increase and range from 150 to 221.63 kJ/mol with an average of 155.76 kJ/mol.

4.3. Evaluation of pre-exponential factor and reaction mechanism

The E_a values obtained by Friedman method are used to predict the reaction mechanism and pre exponential factor using master plots and method of compensation parameters for the process, since the method is found to be more efficient than the rest of isoconversional methods.

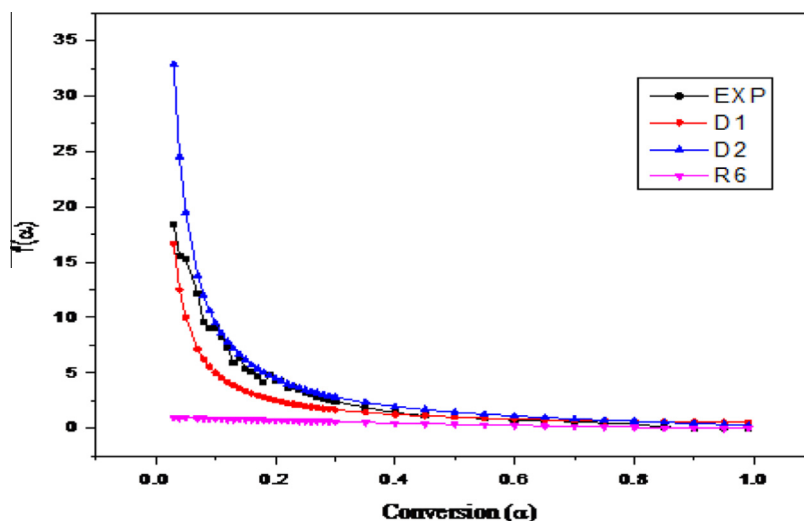
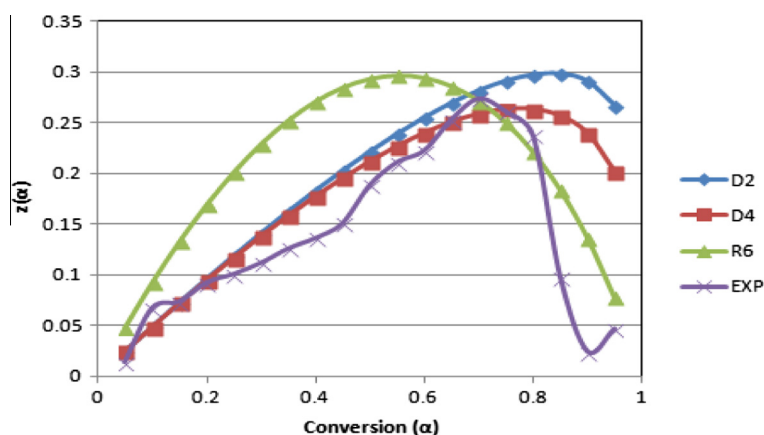
4.3.1. Using compensation parameters

Friedman equation is used for evaluation of E and A values for all the common mechanisms in solid state kinetics given in Table 1 at all six different heating rates. The diffusion and reaction order models give a high regression coefficient ($R > 0.95$) and are used for evaluation of compensation effect parameters for each heating rate. The compensation parameters obtained are $\alpha^* = -5.896$ and $\beta^* = 0.187$ with $R = 0.9912$. These compensation parameters are used for evaluation of A_x at each conversion value using Eq. (15). The $\ln A_x$ values vary in the range of 14–29.43 s^{-1} with an average value of 21.6 s^{-1} . The $f(\alpha)$ is numerically evaluated using A_x and E_x values and is compared against the theoretical $f(\alpha)$ curves. The experimental and theoretical curves for $f(\alpha)$ are shown in Fig. 3a. The experimental curve of pine wood in Fig. 3a overlaps with the D1, D2 curves for conversion values up to 0.7. These mechanisms refer to the diffusion process in one and two dimension, respectively. At conversion values greater than 0.7 the curve is closer to R6 degradation mechanism which refers to reaction order model with order of reaction as 1.5. The overall trend is similar to two dimensional diffusion mechanism (D2).

4.3.2. Using $z(\alpha)$ master plots

The $z(\alpha)$ master plots are shown in Fig. 3b. At conversion values less than 0.3 the experimental curve overlaps the D2 and D4 curves. The experimental curve follows the trend of D2 and D4 curves till a conversion of 0.7. These mechanisms refer to diffusion controlled reactions in two and three dimension, respectively. The D4 curve corresponds to three dimensional diffusion–Ginstling–Brounshtein equation which refers to diffusion controlled reactions starting on the exterior of a spherical particle with radius r_0 . At conversion values greater than 0.7 the trend of curve is similar to that R6 curve corresponding to the reaction order model with order of reaction as 1.5.

The predictions from the method of compensation parameters and $z(\alpha)$ master plots are similar and both predict the similar mechanisms for decomposition reaction of pine wood. The process of pine wood pyrolysis seems to be controlled by diffusion mechanism in a wide conversion region, and is then transferred to the regime controlled by one and half order reaction at higher temperatures. At conversion values greater than 0.7 the mechanism predicted is a reaction of order 1.5. At conversion values less than 0.7 the reaction is controlled by diffusion but the exact predicted mechanism among the diffusion controlled reactions is different predicted from different methods. While the method of compensation parameters suggests a two dimensional diffusion mechanism, the experimental master plots are closer to two dimensional diffusion and three dimensional – Ginstling

Fig. 3a. Experimental and theoretical $f(\alpha)$ curves.Fig. 3b. $z(\alpha)$ master plots for pine wood.

Brounshtein equation. The predictions made by $z(\alpha)$ master plots are made in a model free way and hence the estimations from these plots hold more importance than those using compensation parameters. The diffusion controlled mechanism of wood can be associated with highest degradation of extractives and hemicellulose content that can lead to a high volatility of main wood components at low temperatures and can probably promote acceleration of cellulose degradation by diffusion (Tsai et al., 2007). Bojan and Marija (Jankovic and Jankovic, 2013) studied pine wood pyrolysis and reported similar results of a diffusion controlled mechanism for pine decomposition. They concluded that the pine wood decomposition is governed by three dimensional diffusion – Jander's equation. Similar mechanism was observed by Wang et al. for wood pyrolysis (Wang et al., 2006).

4.4. Isothermal predictions from non-isothermal curves

The kinetic predictions made from isoconversional methods were validated by making isothermal predictions from non-isothermal kinetic data. Isothermal predictions were made using the equation below,

$$t_\alpha = \frac{\int_0^T \exp\left(\frac{-E}{RT}\right) dT}{\beta \exp\left(\frac{-E}{RT_0}\right)} \quad (18)$$

where t_α is the time to reach the extent of conversion α at the temperature T_0 (Burnham and Braun, 1999). For the case of

isoconversional analysis, the sole evaluation of E_α dependence is sufficient to predict the isothermal kinetics from nonisothermal data. The E_α versus α values are used for making isothermal predictions for pine wood sample at 400 °C and the results are compared with the experimental isothermal values. The graph for isothermal prediction is shown in Fig. 4. The theoretical and experimental curves are very close thus validating the kinetic results.

The manuscript aims at generating kinetic data for biomass pyrolysis and exploring its applicability to kinetic models and make meaningful kinetic predictions. The kinetic predictions will help in understanding the complexity of composition with respect to

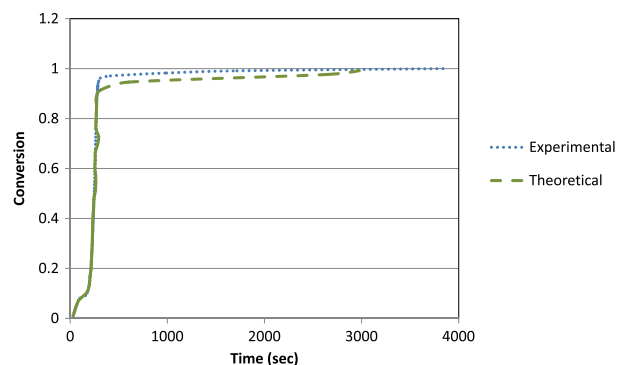


Fig. 4. Isothermal predictions at 400 °C.

activation energy, reaction mechanism etc., which is different for different biomass. The same has been added in the manuscript.

5. Conclusions

Multistep kinetics is detected from isoconversional plot indicating the complex nature of pine wood pyrolysis. Pine wood decomposition mechanism is observed to be governed by a diffusion mechanism up to conversion values of 0.7 and then by a $1\frac{1}{2}$ order reaction. The exact mechanism is unclear but a 2D diffusion mechanism fits well by both the methods in wide range of conversion. Three regimes can be seen from isoconversional plot with E_a of 134.32, 146.89 and 155.76 kJ/mol. The isothermal predictions (400 °C) are in close agreement with the experimental curves and hence validate the kinetic analysis.

Acknowledgements

The authors thank the Director, CSIR-Indian Institute of Petroleum (IIP) for support and encouragement. GM thanks Council of Scientific and Industrial Research (CSIR) for providing fellowship in the form of Trainee Scientist. The authors also thank CSIR for providing financial assistance in the form of CSIR XII FYP BioEn project.

Appendix A. Supplementary data

Supplementary data associated with this article can be found, in the online version, at <http://dx.doi.org/10.1016/j.biortech.2015.01.087>.

References

- Bamford, C.H., Crank, J., Malan, D.H., 1946. The combustion of wood. Part I. Proc. Camb. Philos. Soc. 42, 166–182.
- Burnham, A.K., Braun, R.L., 1999. Global kinetic analysis of complex materials. Energy Fuels 13 (1), 1–22.
- Cendrowska, A., 1997. Hydrolysis kinetics of cellulose of forest and agricultural biomass. Eur. J. Wood Wood Prod. 55 (3), 195–196.
- Czernik, S., Bridgwater, A., 2004. Overview of applications of biomass fast pyrolysis oil. Energy Fuels 18, 590–598.
- Di Blasi, C., 2008. Modeling chemical and physical processes of wood and biomass pyrolysis. Prog. Energy Combust. Sci. 34 (n1), 47–90.
- Fisher, T., Hajaligol, M., Waymack, B., Kellogg, D., 2003. Pyrolysis behavior and kinetics of biomass derived materials. J. Anal. Appl. Pyrol. 62, 331–349.
- Jankovic, B., Jankovic, M., 2013. Pyrolysis of pine and beech wood samples under isothermal experimental conditions.-the determination of kinetic triplets. Cell. Chem. Technol. 47 (9–10), 681–697.
- Koufopoulos, C.A., Mascio, G., Lucchesi, A., 1989. Kinetic modelling of the pyrolysis of biomass and biomass components. Can. J. Chem. Eng. 67 (1), 75–84.
- Lesnikovich, A.I., Levchik, S.V., 1983. A method of finding invariant values of kinetic parameters. J. Therm. Anal. 27, 89–93.
- Matheus, P., Zattera, A.J., Santana, R.M.C., 2012. Thermal decomposition of wood: kinetics and degradation mechanisms. Bio Resour. Technol. 126 (2012), 7–12.
- Milosavljevic, I., Suuberg, E.M., 1995. Cellulose thermal decomposition kinetics: global mass loss kinetics. Ind. Eng. Chem. Res. 34, 1081–1091.
- Sbirrazzuoli, N., 2013. Determination of pre-exponential factors and of the mathematical functions $f(x)$ or $G(x)$ that describe the reaction mechanism in a model-free way. Thermochim. Acta 564, 59–69.
- Shafizadeh, F., Chin, P.P.S., 1977. Thermal deterioration of wood. ACS Symp. Ser. 43, 57–81.
- Tsai, W.T., Lee, M.K., Chang, Y.M., 2007. Fast pyrolysis of rice husk: product yields and compositions. Bioresour. Technol. 98, 22–28.
- Vyazovkin, S., 2000. Computational aspects of kinetic analysis. Part C. The ICTAC kinetics project – the light at the end of the tunnel? Thermochim. Acta 355, 155–163.
- Vyazovkin, S., Sbirrazzuoli, N., 2006. Isoconversional kinetic analysis of thermally stimulated processes in polymers. Macromol. Rapid Commun. 27, 1515–1532.
- Vyazovkin, S., Burnham, A., Criado, J., Maqueda, L., Popescu, C., Sbirrazzuoli, N., 2011. ICTAC Kinetics Committee recommendations for performing kinetic computations on thermal analysis data. Thermochim. Acta 520, 1–19.
- Wang, J., Wang, G., Zhang, M., Chen, M., Li, D., Min, F., Chen, M., Zhang, S., Ren, Z., Yan, Y., 2006. A comparative study of thermolysis characterization and kinetics of seaweeds and fir wood. Process Biochem. 41, 1883–1886.